Available online at www.sciencedirect.com
ScienceDirect
Journal of Power Sources 174 (2007) 838–842
JOURNAL OF POWER SOURCES
www.elsevier.com/locate/jpowsour

Short communication

Charge–discharge characteristics of all-solid-state thin-filmed lithium-ion batteries using amorphous Nb_2O_5 negative electrodes

Hiromi Nakazawa [b,*], Kimihiro Sano [a], Takashi Abe [a], Mamoru Baba [b], Naoaki Kumagai [b]

[a] *Research and Development Center, Geomatec Co. Ltd., 9 Obasamakananuma, Kannari, Kurihara, Miyagi 989-5184, Japan*
[b] *Graduate School of Engineering, Iwate University, 4-3-5 Ueda, Morioka 020-8551, Japan*

Available online 3 July 2007

Abstract

All-solid-state thin-filmed lithium-ion rechargeable batteries composed of amorphous Nb_2O_5 negative electrode with the thickness of 50–300 nm and amorphous $Li_2Mn_2O_4$ positive electrode with a constant thickness of 200 nm, and amorphous $Li_3PO_{4-x}N_x$ electrolyte (100 nm thickness), have been fabricated on glass substrates with a 50 mm × 50 mm size by a sputtering method, and their electrochemical characteristics were investigated. The charge–discharge capacity based on the volume of positive electrode increased with increasing thickness of negative electrode, reaching about 600 mAh cm^{-3} for the battery with the negative electrode thickness of 200 nm. But the capacity based on the volume of both the positive and negative electrodes was the maximum value of about 310 mAh cm^{-3} for the battery with the negative electrode thickness of 100 nm. The shape of charge–discharge curve consisted of a two-step for the batteries with the negative electrode thickness more than 200 nm, but that with the thickness of 100 nm was a smooth S-shape curve during 500 cycles.

Keywords: Li-ion battery; Thin-filmed solid-state battery; Amorphous electrode; $Li_2Mn_2O_4$; Nb_2O_5

1. Introduction

Recently, much attention has been paid to the investigations of solid-state lithium-ion rechargeable batteries and lithium-metal-free batteries [1–6]. If such a rocking-chair type of battery is constructed with only a thin-filmed type of electrodes and electrolyte, it will be very compact, light and highly reliable, and therefore we can find widespread application in many types of portable electronic devices. As one of such batteries, we have developed a thin-filmed lithium-ion rechargeable battery fabricated using a sputtering method [6]. It was composed of a thin-filmed $LiMn_2O_4$ positive electrode, a V_2O_5 negative electrode, a $Li_3PO_{4-x}N_x$, so-called LIPON electrolyte [2], and V films as an electric collector. The cell size was 1 cm^2 in area and about 2.2 μm in thickness, and it showed a good charge–discharge performance with a capacity of about 18 μAh.

But the charge–discharge capacity is too small to drive practical electronic devices, so that we recently have accomplished large-sized and thin-filmed lithium-ion rechargeable batteries of which the typical cell size was 100 mm × 100 mm in area and about 3.1 μm in thickness by using amorphous $Li_2Mn_2O_4$ positive electrode, V_2O_5 negative electrode, and LIPON electrolyte films [7]. The reason to use amorphous films is to prevent a crack and a peeling by stress that grows largely in crystallized film as the size and thickness of the cell increase. The battery showed good charge and discharge characteristics with a typical capacity of about 0.9 mAh and it could drive a digital watch as a portable device for more than 1 month with only one time charging.

However, the charge–discharge curve of the battery using a V_2O_5 negative electrode is not flat and the voltage decreased rapidly with discharge [7]. Moreover the V_2O_5 has toxicity. In addition, the charge–discharge capacity of the thin-filmed battery is not enough yet to drive portable devices in comparison with normal battery with a liquid electrolyte. So, it is expected to improve the charge–discharge characteristics and to increase the capacity by using other negative electrode materials instead of V_2O_5.

We examined charge–discharge properties of the several thin-filmed batteries composed of various negative electrodes and a $Li_2Mn_2O_4$ positive electrode, and found that Nb_2O_5 can be used as a suitable thin-filmed negative electrode. In present work, we report charge–discharge properties of thin-filmed batteries

* Corresponding author. Tel.: +81 19 621 6387; fax: +81 19 621 6387.
E-mail addresses: nakazawa@frontier.iwate-u.ac.jp (H. Nakazawa), baba@frontier.iwate-u.ac.jp (M. Baba).

0378-7753/$ – see front matter © 2007 Published by Elsevier B.V.
doi:10.1016/j.jpowsour.2007.06.226

having amorphous Nb_2O_5 thin films with different thicknesses as a negative electrode.

2. Experimental

Using a DC/RF magnetron sputtering equipment, of which chamber size was 800 mm in diameter and in which four targets were installed, lithium-ion rechargeable batteries were fabricated on glass substrates installed in the chamber as follows [7]. First, on a glass substrate (50 mm × 50 mm in area and 1.1 mm in thickness), a V metal current collector film was deposited by a dc-magnetron sputtering method (DC method) from a V metal target with a typical dc power of 1.0 kW and an Ar-gas pressure of 2.0 mTorr. The film thickness was 100 nm. Next, a thin film of positive electrode was deposited on it by an rf-magnetron sputtering method (RF method) from a $Li_2Mn_2O_4$ sintered target with a typical power of 1.2 kW in a mixture gas of Ar and O_2 (9:1). The gas pressure was 3.0 mTorr and the film thickness was 200 nm. Then, a thin film of solid $Li_3PO_{4-x}N_x$ electrolyte (100 nm) was deposited by using the RF method from a Li_3PO_4 sintered target in N_2 gas. After that, a negative electrode was deposited by using the RF method from a Nb_2O_5 sintered target with a power of 1.0 kW in a mixture gas of Ar and O_2 (9:1). Finally, a V film (100 nm) was deposited again by using the DC method. The thickness of Nb_2O_5 negative electrode was changed from 50 to 300 nm to optimize the thickness. These films were all deposited at room temperature without heating the glass substrate. An effective cell size was 32 mm × 32 mm in area. A schematic diagram of the thin-filmed battery in a cross-section is shown in Fig. 1, and a photograph of the plane view is shown in Fig. 2.

The crystal structures of those films were investigated by XRD measurement. No XRD peaks were observed for any film, confirming that all these films were in an amorphous state. Here, the chemical compositions of the deposited films were indicated by those of the used targets such as Nb_2O_5 and $Li_2Mn_2O_4$.

Charge–discharge properties of these batteries were measured at room temperature with a current of 0.02–0.10 mA between 3.5 and 0.3 V by using a charge–discharge measuring instrument.

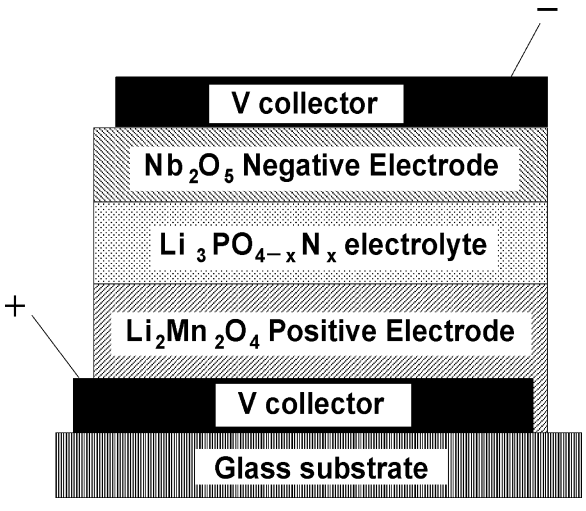

Fig. 1. A schematic diagram of the thin-filmed $Nb_2O_5/Li_2Mn_2O_4$ battery in a cross-section.

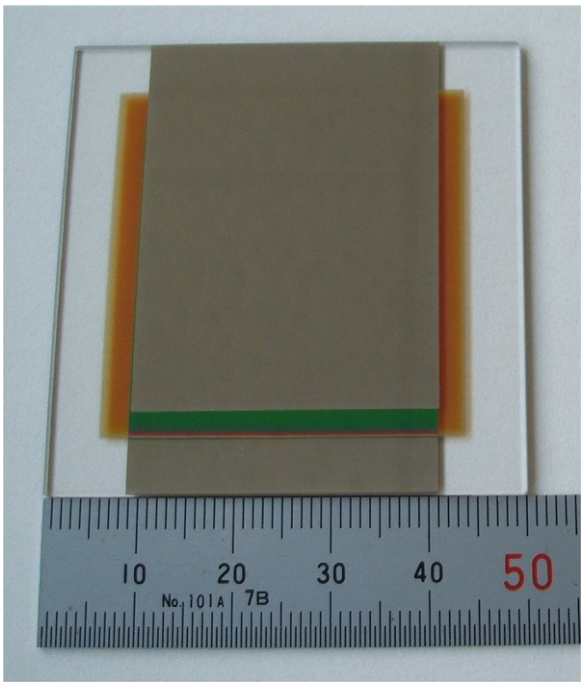

Fig. 2. A photograph of the thin-filmed battery with a 50 mm × 50 mm size in a plane view.

3. Results and discussion

Fig. 3(a)–(d) shows the charge–discharge characteristics of the batteries having Nb_2O_5 negative electrode with different thicknesses and a $Li_2Mn_2O_4$ positive electrode at a current of 0.02 mA. Here, the charge–discharge capacities were obtained based on the volume of positive electrode in those batteries. As generally observed in any battery, the initial charge capacity exceeded the following discharge one, showing a considerable irreversibility. The irreversible capacities at the Nb_2O_5 thicknesses of 200 nm (c) and 300 nm (d) are larger than those at the thicknesses of 50 nm (a) and 100 nm (b). After the 2nd cycle, steady cycling behaviors are observed. This may be attributed to the fact that a considerable amount of Li is trapped in the negative electrode as irreversible Li during the 1st cycle. As seen in Fig. 3, at initial stage of the first charge process the voltage once decreased rapidly, then increasing with capacity. This is probably attributed to intrinsic property of Nb_2O_5 thin film.

The charge–discharge curves consist of smooth S-shape profile at any cycle without any plateau for the negative electrode with smaller thicknesses of 50 and 100 nm ((a) and (b)). At higher thickness of 200 nm, however, a shoulder appears and it grows with cycling (c). Moreover, for the larger thickness of 300 nm, a two-step variation clearly appears with cycling (d).

The appearance of the two-step voltage variation at a higher Nb_2O_5 thickness would be due to the structural variation of amorphous $Li_2Mn_2O_4$ positive electrode [8–10]. The prepared $Li_2Mn_2O_4$ film is in an amorphous state from XRD measurement. The average discharge potential of crystalline $Li_2Mn_2O_4$

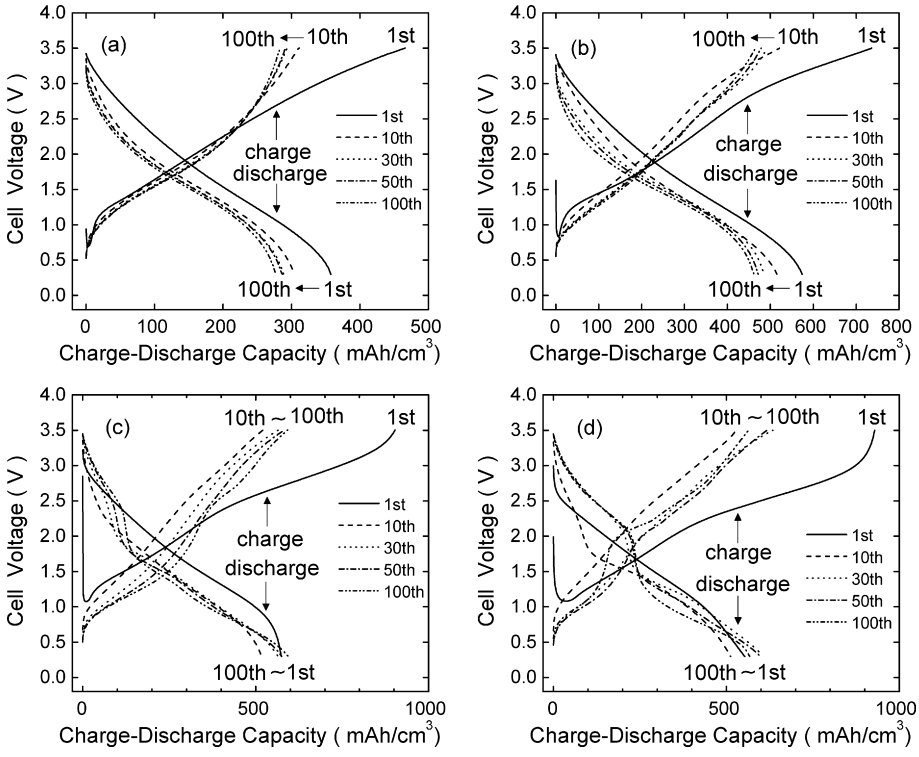

Fig. 3. Charge–discharge characteristics of the batteries having Nb_2O_5 negative electrodes with different thicknesses: (a) 50 nm, (b) 100 nm, (c) 200 nm, and (d) 300 nm.

($LiMnO_2$) is about 3.3 V versus Li/Li^+ and the potential changes in the range of 2.0–4.5 V versus Li/Li^+ on cycling [11,12]. The prepared Nb_2O_5 negative electrode has also amorphous structure and the average discharge potential is about 1.6 V versus Li/Li^+ [3,13], and the potential smoothly changes in the range of 1.0–2.6 V versus Li/Li^+ on discharge. Thus, the 1st charge–discharge profile of $Nb_2O_5/Li_2Mn_2O_4$ battery becomes a smooth S-shape curve having average voltage of about 1.7 V and the voltage may vary in broad voltage range of 3.5–0.3 V, with cycling.

On the other hand, the high crystalline spinel-related $LiMn_2O_4$, normally prepared by high-temperature calcination, shows a two-step discharge profile at the potential of 3 and 4 V due to the two kinds of the crystallographic sites of tetrahedral 8a and octahedral 16c for lithium incorporation [14]. As can be seen in Fig. 3, the stepwise discharge curves appear with increasing thickness in the Nb_2O_5 electrode and also with increasing cycling number. This indicates that during a charging process more amounts of Li were removed from the $Li_2Mn_2O_4$ electrode with increasing thickness of Nb_2O_5 films, reaching to the composition of $Li_{1-x}Mn_2O_4$ ($x<1$). A considerable amount of Li remained in the Nb_2O_5 electrode during the initial discharge, leading to the larger irreversible capacity with increasing Nb_2O_5 thickness. The much amount of Li removal from amorphous $Li_2Mn_2O_4$ may form spinel-related crystal domain in the amorphous structure [9,12]. This may create the tetrahedral 8a site showing a high Li insertion potential of about 4 V. Thus, the clearer two-step discharge voltage profile would appear with increasing Nb_2O_5 film thickness and increasing cycling number. We are now investigating the electrochemical behavior and structural variation of single $Li_2Mn_2O_4$ and Nb_2O_5 film electrodes. The experimental results will be reported elsewhere.

For the $Nb_2O_5/Li_2Mn_2O_4$ battery, the discharge voltage is higher than that of $V_2O_5/Li_2Mn_2O_4$ battery [7]. Practically, the voltage more than 1.0 V is necessary to drive electric devices such as digital watch using liquid crystal even if they consume low electric power. For the battery with V_2O_5 negative electrode, the ratio of the capacity at the working voltage of 1.0–3.5 V compared to the total capacity between 0.3 and 3.5 V is 30% [7]. While the ratio is about 80% for the batteries with a thinner Nb_2O_5 negative electrode (thickness: 50–100 nm) and it is about 50–60% for those with a thicker Nb_2O_5 negative electrode (thickness: 200–300 nm), as seen in Fig. 3. Thus, Nb_2O_5 is found to be more profitable negative electrode for the thin-filmed batteries in comparison with V_2O_5 negative electrode, and the battery with a Nb_2O_5 negative electrode of the thickness of 100 nm shows especially excellent charge–discharge performance.

Fig. 4(a) shows cycle performances on the discharge capacities at a current of 0.02 mA. The capacities were obtained based on the volume of positive electrode in those batteries. For the batteries having Nb_2O_5 negative electrode thicknesses of 50 and 100 nm, the capacities gradually decreased during 30 cycles, then being almost constant with about 300 and 480 mAh cm^{-3}, respectively. For the thicknesses of 200 and 300 nm, the capacities decreased until about 10th cycle, then increased. After 20–30 cyclings, they reached almost constant capacity of about 600 mAh cm^{-3} for both the thicknesses. Such a battery behavior would correspond to appearance of a shoulder shown in Fig. 3, as discussed above. In comparison with V_2O_5, the capacities of

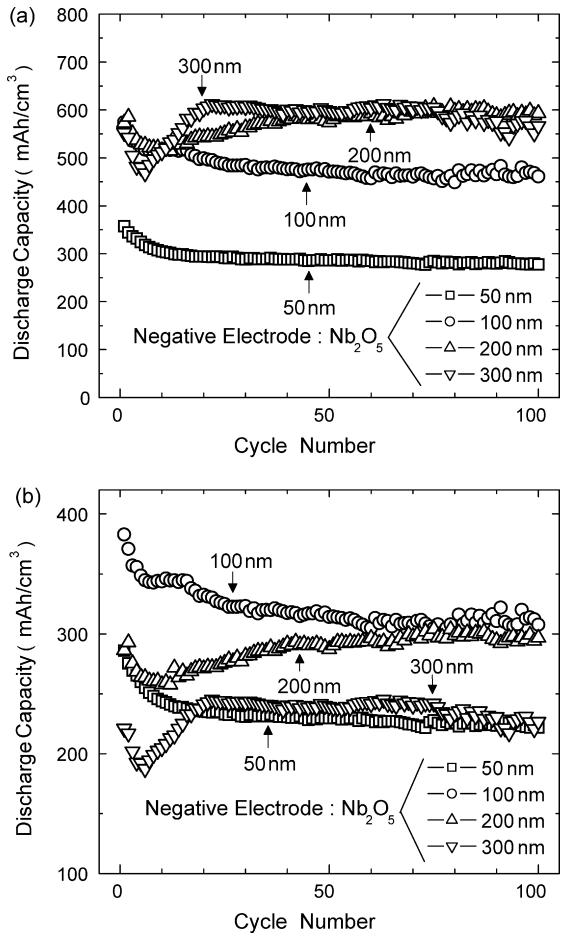

Fig. 4. Cycle performances of the batteries with different Nb_2O_5 electrode thicknesses: (a) the capacity is based on the volume of positive electrode and (b) the capacity is based on the volume of both positive and negative electrodes at a current of 0.02 mA.

300–600 mAh cm^{-3} based on the volume of positive electrode for a Nb_2O_5 negative electrode are larger than that of about 180 mAh cm^{-3} for a V_2O_5 negative electrode [7].

The capacity increases as the negative electrode thickness increases until the thickness of 200 nm, and the capacity with 300 nm is almost same as that with 200 nm, as seen in Fig. 4(a). This is attributed to that the capacity on the $Li_2Mn_2O_4$ positive electrode with the constant thickness of 200 nm corresponds to the capacity on the Nb_2O_5 negative electrode with the thickness of 200 nm. Thus the amount of $Li_2Mn_2O_4$ electrode limits the capacity of the present battery system.

Fig. 4(b) shows cycle performances on the discharge capacities based on the volume of both the positive and negative electrodes in the batteries. The stable capacity of the battery with the negative electrode thickness of 100 nm is about 310 mAh cm^{-3}, which is largest among all the batteries during 100 cycles. The batteries with negative electrode thicknesses of 50 and 300 nm show smaller capacity of about 230 mAh cm^{-3}. These capacities of 230–310 mAh cm^{-3} based on the volume of both positive and negative electrodes for a Nb_2O_5 negative electrode is larger than that of about 130 mAh cm^{-3} for the battery with V_2O_5 negative electrode [7].

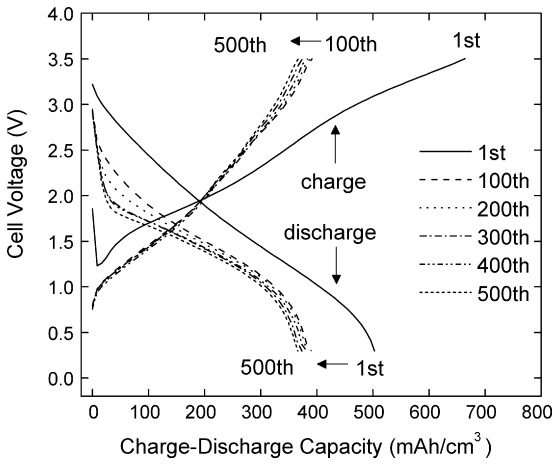

Fig. 5. Charge–discharge characteristics of the battery with a Nb_2O_5 negative electrode with a thickness of 100 nm at a current of 0.10 mA until 500 cycles.

In application to practical devices, it is important to increase the capacity based on a volume, or a cell thickness of the film battery, nearly corresponding to the capacity based on the volumes of positive and negative electrodes, because the thicknesses of electric collector and solid electrolyte are nearly constant regardless of the thicknesses of positive and negative electrodes. So, the negative electrode thicknesses of 100 and 200 nm are suitable for application to realistic devices. Especially, the Nb_2O_5 negative electrode with the thickness of 100 nm is more favorable from the stability of the charge–discharge curve, as seen in Fig. 3.

Fig. 5 shows the charge–discharge characteristics of the battery consisting of a Nb_2O_5 negative electrode with the thickness of 100 nm at a current of 0.10 mA during prolonged 500 cycles. The charge–discharge capacities were obtained based on the volume of positive electrode. At early stage of the initial charging, the voltage once decreased and then increased, and the initial charge capacity exceeds the following discharge one. After the 2nd cycle, the discharge capacity almost agrees with the charge one. These phenomena are similar to the case at a current of 0.02 mA shown in Fig. 3(b). The stable charge–discharge curve

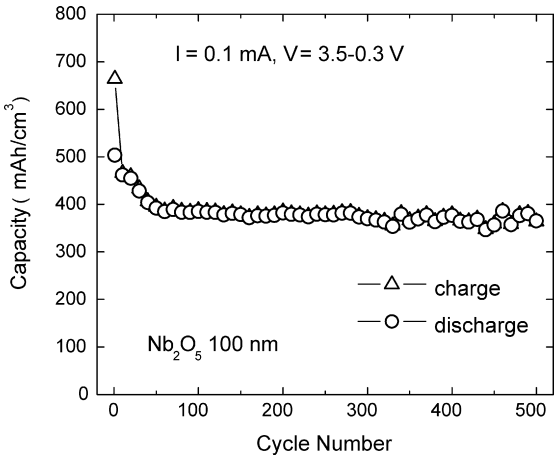

Fig. 6. Cycle performance of the battery with a Nb_2O_5 negative electrode with a thickness of 100 nm at a current of 0.10 mA until 500 cycles.

consisting of a smooth S-shape curve without any shoulder was obtained on prolonged cyclings.

Fig. 6 shows cycle performance of the battery with a Nb_2O_5 negative electrode (100 nm thickness) at a current of 0.10 mA during 500 cycles. The capacities were obtained based on the volume of positive electrode. Until about 50 cycles the capacities decrease gradually to the capacity of 400 mAh cm^{-3}, then retaining almost a constant capacity of 400 mAh cm^{-3} during 500 cycles. This capacity of 400 mAh cm^{-3} is a little smaller in comparison with that of 480 mAh cm^{-3} at a current of 0.02 mA. So this battery using a Nb_2O_5 negative electrode with 100 nm thickness is found to show a fairly stable performance for prolonged cycling at higher current of 0.10 mA.

4. Summary

We have investigated the electrochemical characteristics of all-solid-state thin-filmed lithium-ion rechargeable batteries composed of amorphous Nb_2O_5 negative electrode with various thicknesses, $Li_2Mn_2O_4$ positive electrode with constant thickness of 200 nm and LIPON electrolyte. The battery performance depended on the negative electrode thickness, resulting in different charge–discharge curves, capacities per unit volume, and cyclic performances. The batteries with a negative electrode thicker than 200 nm showed an unstable cycling behavior consisting of a two-step curve, while the batteries with a negative electrode thinner than 100 nm showed a stable cycling curve characterized by an S-shape as the cycle goes on. Especially, the battery with the Nb_2O_5 negative electrode of the thickness of 100 nm showed most favorable charge–discharge properties with the capacity of 310–380 mAh cm^{-3} based on the volume of both the positive and negative electrodes, and with stable cycling curve for 500 times.

Acknowledgments

We would like to thank R. Jinnouchi and S. Tsuruta for their experimental assistance.

References

[1] S.D. Jones, J.R. Akridge, Solid State Ionics 53–56 (1992) 628.
[2] J.B. Bates, N.J. Dudney, G.R. Gruzalski, R.A. Zuhr, A. Choudhury, C.F. Luck, J. Power Sources 43–44 (1993) 103.
[3] N. Kumagai, Y. Tateshita, Y. Takatsuka, M. Baba, T. Ikeda, K. Tanno, J. Power Sources 54 (1995) 175.
[4] N. Kumagai, H. Kitamoto, M. Baba, S. Durand-Vidal, D. Devilliers, H. Groult, J. Appl. Electrochem. 28 (1998) 41.
[5] M. Baba, N. Kumagai, H. Kobayashi, O. Nakano, K. Nishidate, Electrochem. Solid State Lett. 2 (1999) 320.
[6] M. Baba, N. Kumagai, N. Fujita, K. Ohta, K. Nishidate, S. Komaba, H. Groult, D. Devilliers, B. Kaplan, J. Power Sources 97–98 (2001) 798.
[7] H. Nakazawa, K. Sano, M. Baba, J. Power Sources 146 (2005) 758.
[8] R.J. Gummow, D.C. Liles, M.M. Thackeray, Mater. Res. Bull. 28 (1993) 1249.
[9] Y. Shao-Horn, S.A. Hackney, A.R. Armstrong, P.G. Bruce, R. Gitzendanner, C.S. Johnson, M.M. Thackeray, J. Electrochem. Soc. 146 (1999) 2404.
[10] J.N. Reimers, E.W. Fuller, E. Rossen, J.R. Dahn, J. Electrochem. Soc. 140 (1993) 3396.
[11] R.J. Gummow, M.M. Thackeray, J. Electrochem. Soc. 141 (1994) 1178.
[12] M.M. Thackeray, C.S. Johnson, A.J. Kahaian, K.D. Kepler, J.T. Vaughey, Y. Shao-Horn, S.A. Hackney, J. Power Sources 81–82 (1999) 60.
[13] T. Ohzuku, K. Sawai, J. Power Sources 19 (1987) 287.
[14] T. Ohzuku, M. Kitagawa, T. Hirai, J. Electrochem. Soc. 137 (1990) 769.